

## Low Velocity-Ratio Pitched and Skewed Jet in a Turbulent Boundary Layer

J. W. Jewkes<sup>1</sup> and Y. M. Chung<sup>2</sup>

<sup>1</sup>Fluid Dynamics Research Group  
Curtin University of Technology, Perth, 6845, Australia

<sup>2</sup>School of Engineering and Centre for Scientific Computing  
University of Warwick, Coventry, CV4 7AL, U.K.

### Abstract

The jet in cross-flow (JICF) is a commonly studied flow in the context of boundary layer control. Particularly, pitched and skewed jets has potential for flow separation control. In this study, both the perpendicular and the pitched and skewed jets were considered to highlight the different flow structures. The formation of the vortical 'shell' was clearly seen in a low velocity-ratio perpendicular JICF, while no such structure was observed in the pitched and skewed case. Instantaneous and time-averaged flow field were analysed in this paper.

### Introduction

A steady jet acting perpendicular to a turbulent boundary layer is frequently encountered in many engineering applications with applications ranging from the flow of pollutants issuing from smokestacks, to V/STOL aeroplanes. Our interest in the jet in cross-flow (JICF) was driven by its potential application in boundary layer control devices, where jets can be used to produce streamwise vortices, similar to solid vortex generating devices. Vortex generating vanes are often seen utilised on modern airliner wings to delay flow separation [1, 2]. Corkscrew vortices generated by these vanes advect downstream, parallel to the wall, mixing and transporting freestream momentum across the boundary layer, which in turn energises the near-wall flow. These solid vortex generating devices are useful under high-lift flow conditions (*e.g.*, aircraft take-off and landing). However, they generate unwanted parasitic drag during level cruise and are therefore poorly suited to active control. Instead, vortex generating jets (VGJ) can be used to generate similar streamwise structures while they can be pulsed (and also pitched and skewed), or varied in velocity according to requirement.

The main parameters governing the behaviour of these jets are the pitch ( $\phi$ ) and skew ( $\theta$ ) angles, and the velocity ratio ( $VR$ ) between the jet and the free-stream. Typical investigations range from  $VR = 0.5$  to  $VR = 10$ , with orifice diameters of the order of the boundary-layer thickness [3–6]. High velocity ratio jets ( $VR \geq 2$ ) have been extensively studied. It was found that the centreline jet trajectory projects away from the wall, penetrating the boundary layer. Shear forces fold the spanwise faces over themselves to form a counter-rotating vortex pair (CVP). The near-wall flow behind the jet is unsteady, and are similar to that produced by a solid cylindrical obstruction.

On the other hand, the low  $VR$  configuration ( $VR < 2.0$ ) has received limited attention, and there appear to be no numerical investigations. The jet centreline remains closer to the wall, well within the boundary layer [4], too close to produce well-defined wake structures. At lower velocity ratios, the wake region of the jet is fundamentally different. Gopalan et al. [7] found that a semi-cylindrical vortical region forms behind the jet, enclosing a region with slow reverse flow originating from the jet shear-layer at  $VR = 1$ .

A pitched and skewed jet has attracted particular interest due

to the boundary layer separation control application. Johnston [8] found that, compared to a trailing vortex pair from a perpendicular jet, a dominant vortex from a pitched and skewed jet interaction is much stronger and appears to provide much more effective momentum transfer across the wall boundary layer. Compton and Johnston [9] reported that a jet pitched by  $45^\circ$  and skewed by  $90^\circ$  tends to form a dominant, 'single' vortex, rather than a CVP. This configuration was first derived by Wallis [10]. Rixon and Johari [11] argued that the pitched and skewed jet creates a counter-rotating vortex pair near the orifice exit, one of which being significantly stronger than the other. Zhang and Collins [12] observed that the weaker secondary vortex dissipated within  $10D$  (where  $D$  is the orifice diameter). Low velocity ratios were used in Compton and Johnston [9] ( $VR \leq 1.3$ ) and Zhang and Collins [12] ( $0.5 \leq VR \leq 1.5$ ) while the jets used by Rixon and Johari [11] crossed the velocity ratio threshold at  $1 \leq VR \leq 3$ . The formation of the vortex shell seen in the perpendicular cases was not observed. The main objectives of this study is to investigate the flow structures associate with a low  $VR$ , pitched and skewed JICF numerically.

### Numerical Method

Results presented in this paper have been computed using a second-order finite volume code [13, 14]. The convective terms were modelled using a third order Runge-Kutta method, and the diffusive terms using Crank-Nicolson method. A fractional-step time-advancement was used and a dynamic subgrid-scale model was applied to calculate the Smagorinsky constant. Length scales were non-dimensionalised with respect to  $\delta_{int}^*$ , velocities with respect to  $U_\infty$ ;  $Re_{\delta^*} = U_\infty \delta^* / \nu = 2000$  at the inlet, where  $\nu$  is the kinematic viscosity. The simulation domain had dimensions  $128\delta^* \times 32\delta^* \times 4\pi\delta^*$  in streamwise ( $x$ ), wall normal ( $y$ ) and spanwise ( $z$ ) directions. Grid resolutions were  $200 \times 60 \times 96$  points, yielding  $\Delta x^+ = 59$ ,  $\Delta y_{wall}^+ \approx 1.2$ , and  $\Delta z^+ = 18$ , uniform in  $x$  and  $z$ , and applying hyperbolic tangent stretching in the wall-normal direction.  $Re_\theta \approx 1500$  at the inlet,  $Re_\theta \approx 1950$  at the domain exit. Inlet boundary conditions were provided by a precursor simulation based on a variant of the Lund et al. [15] formulation. More details are described in [16]. Upper boundary conditions were  $u = U_\infty$ ,  $\partial v / \partial y = 0$ ,  $\partial w / \partial y = 0$ , the spanwise domain boundary was periodic, and the exit plane used a convective boundary condition.

### Perpendicular Jet

The  $VR = 1$  perpendicular jet was located on the spanwise centreline,  $x_{jet} = 48\delta^* (\approx 6\delta)$  downstream of the domain inlet, (37.5% of the streamwise domain length, corresponding to  $Re_\theta \approx 1650$  in the flat plate case), with a circular orifice of diameter  $D = 4\delta^* (\approx 0.5\delta)$ . The grid resolution of the jet corresponding with the existing rectilinear grid described above, yielding  $6 \times 31$  nodes across the jet. The jet velocity profile was provided by a hyperbolic tangent function taken from Chung

et al. [17].

$$u_{jet} = \frac{1}{2} \left[ 1 + \tanh \left( \frac{0.5 - |x|/D}{2\theta_{jet}} \right) \right], \quad (1)$$

Where  $|x|$  represents position across the jet from the jet centreline,  $\theta_{jet}$  representing the momentum thickness of the jet inflow, where the ratio of momentum thickness to the jet diameter;  $D/\theta_{jet} = 20$ .

Figure 1 illustrates the formation of this vortical ‘shell’ for a low velocity-ratio perpendicular JICF. It occurs because the up-stream and downstream edges of the jet experience different conditions as the jet emerges from the orifice. Essentially the rear, downstream face of the jet is shielded from the free-stream by the jet itself, while the upstream face is exposed directly to the crossflow. The sides experience the fastest streamwise flow, due to the ‘blockage’ caused by the jet - in much the same way as the high  $VR$  cases. At low velocity ratios, the vorticity at the leading face of the jet is dissipated by the boundary layer. The jet vortex ring is stretched along the rear face, which subsequently ‘peels over’ to enclose the region of slow-moving fluid, leading to the semi-cylindrical shell behind the jet. Meyer et al. [18] also investigated a  $VR = 1.3$  perpendicular jet, and argued that the vortical shell layer in actual fact contains a steady pair of rotationally opposed tornado-like vortices. This is fundamentally different from the high  $VR$  case, where the higher jet momentum at the leading edge is strong enough to overcome dissipation, and allows the jet column to coherently bend away from the wall. In this case, the jet vorticity (although distorted), remains confined to the jet forming the counter-rotating vortex pair.

Figure 2 shows the mean velocity magnitude ( $\sqrt{(U^2 + V^2)}$ ) and streamlines at spanwise ( $z$ ) jet centreline. There is a region of weak reverse-flow behind the jet, persisting until  $x/D = 3$  (see also Figure 3). Clearly a strong shear-layer persists along the rear face of the jet, but along the leading edge, the mean shear diminishes quickly, vanishing by  $x/D \approx 1$  (slightly lower than in the experimental case).

Figure 3 shows an  $xz$  velocity contour plot and streamlines for the time-averaged  $\sqrt{(U^2 + W^2)}$  at a wall normal distance of

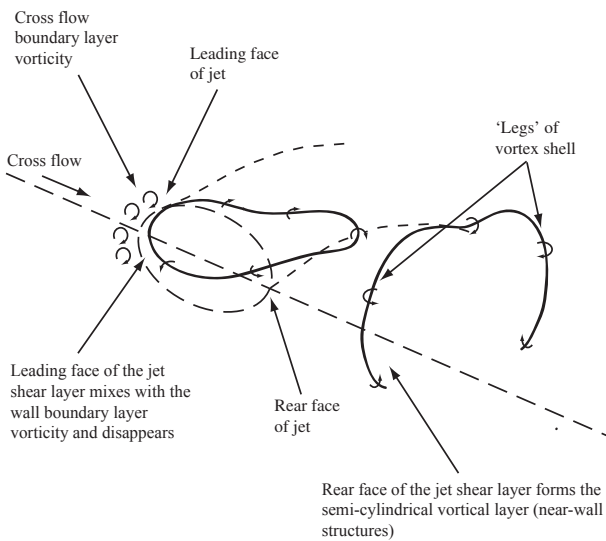


Figure 1: Illustration of the mechanism behind the formation of the semi-cylindrical vortical layer behind the jet at low  $VR$  perpendicular JICF (based on Gopalan et al. [7]).

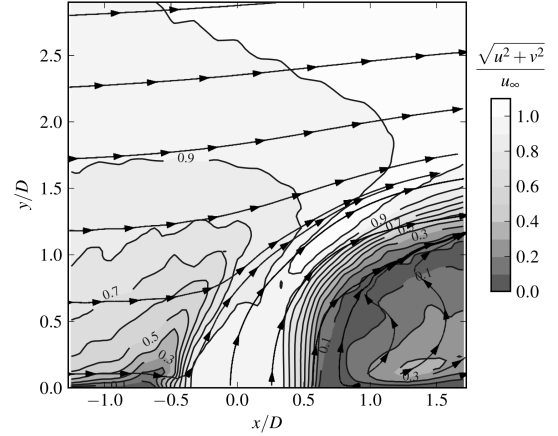


Figure 2: Mean velocity  $\sqrt{(U^2 + V^2)}$  contour plots and streamlines at the jet centreline.

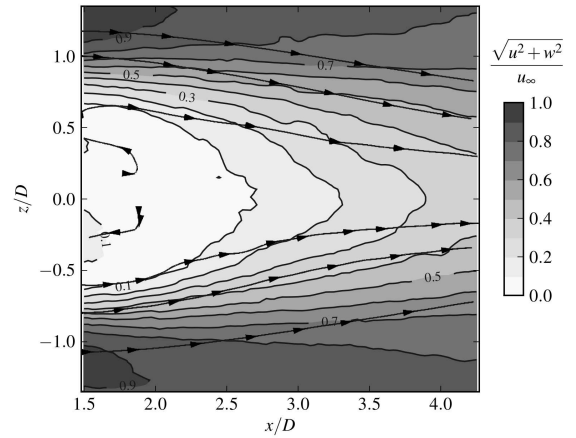


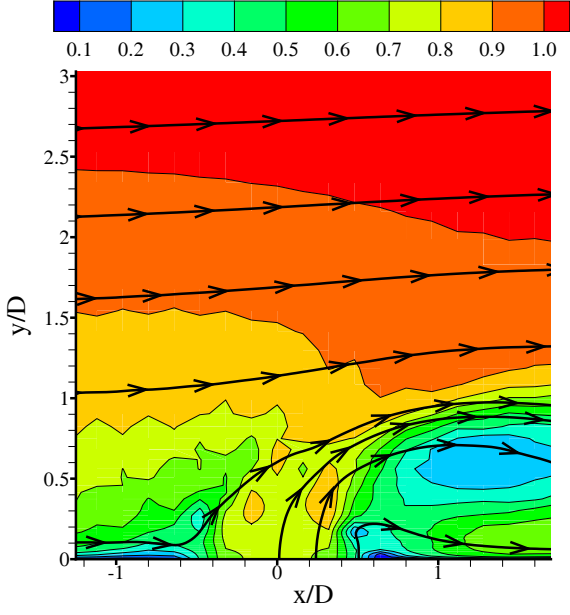
Figure 3: Mean velocity  $\sqrt{(U^2 + W^2)}$  contour plots and streamlines at  $y/D = 0.6$ .

$y/D = 0.6$ . Again, there is agreement with the experimental results, with a region of reversed flow extending up to  $x/D \approx 2.0$ . Meyer et al. [18] argued that this vortical shell layer in actual fact contains a steady pair of tornado-like vortices, and the reverse-flow streamlines in our plot seem to support this.

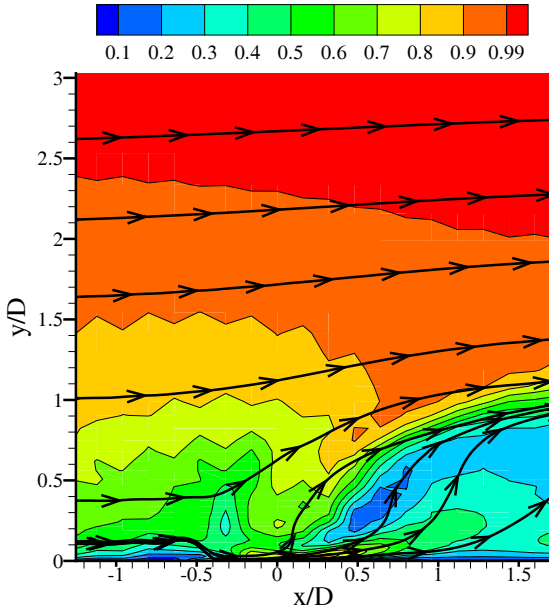
Time-averaged contour fields of a  $VR = 1$  perpendicular jet compared well with the experimental work of Gopalan et al. [7]. Please note that their experimental data was produced using PIV at  $Re_\theta \approx 6100$  and  $D \approx 0.35\delta$ . Despite these differences in  $Re$  number and orifice size, the figures demonstrate good agreement between our numerical results and the experimental data.

### Pitched and Skewed Jet

Here, we present the pitched and skewed case. It is worth noting that despite the perpendicular case demonstrating signs of the formation of a vortex ‘shell’ behind the jet, (containing weak reverse flow), no mention has been made of this being the case in the pitched and skewed configuration. Indeed authors usually describe the formation of a single, coherent streamwise vortex, even in the low  $VR$  cases. It is instructive to compare Figure 4a



(a)



(b)

Figure 4: Mean velocity  $\sqrt{(U^2 + V^2)}$  contour plot and streamlines for the pitched and skewed case. (a) at the jet centreline, and (b) at an offset of  $z = 0.6D$ .

with Figure 2. There seems to be reasonable qualitative agreement between the two cases in terms of the diminished velocity at the leading edge of the jets, however the wake of the jet does not show any signs of the reverse-flow shown in the perpendicular JICF case. An offset velocity contour plot, placed at  $z = 0.6D$  in the 'core' of the wake of the pitched and skewed jet, is presented in Figure 4b. When compared with figure 4a, it becomes clear that there appears to be no indication of the reverse flow seen in the perpendicular case.

A vorticity contour plot of mean  $\omega_z$  at the jet centreline (not

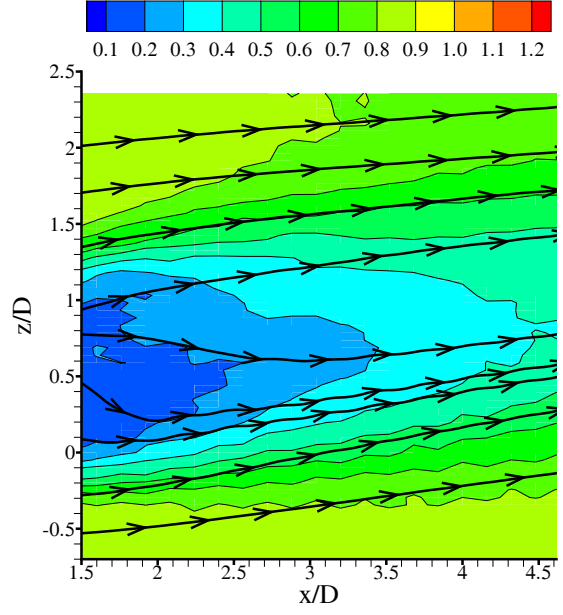


Figure 5: Mean velocity  $\sqrt{(U^2 + W^2)}$  contour plots and streamlines at  $y/D = 0.6$ .

shown here) shows diminished positive vorticity at the leading edge, and stronger negative vorticity at the trailing edge of the jet, indicating vorticity dissipation at the leading edge. The pitch and skew of the jet makes it difficult to capture the wake region in this centreline plot, but it is worth noting that the pitched and skewed wake appears to sit closer to the wall than in the perpendicular case.

Figure 5 shows a velocity contour plot and streamlines for mean  $\sqrt{(U^2 + W^2)}$  in the  $xz$  plane at  $y/D = 0.6$ , which should be compared to Figure 3. Please note the  $z$  axis offset for the pitched and skewed case. Despite the perpendicular jet showing signs of weak reversed  $u$  velocity at a number of stations in the jet's wake, the pitched and skewed case merely indicates a reduction in centreline velocity. We can see evidence of the formation of a vortex shell with a region of weak reverse  $u$  velocity in the perpendicular jet case, with two spatially separated shear-layers within this shell. The pitched and skewed case however seems to indicate some slowing of the  $u$  velocity centreline, but no reverse flow. Furthermore, there appears to be evidence of just one streamwise rotating structure behind the jet.

Earlier we had mentioned that authors studying these pitched and skewed low  $VR$  jets had made no mention of the 'shell' structure seen in the perpendicular cases. Our results appear to support this, we can see no region of reversed flow, and the results appear to show signs of the formation of a coherent streamwise vortex, consistent with the experimental observations of Rixon and Johari [11] and Compton and Johnston [9]. Figure 6 highlights this, the velocity streamlines seeded from a position  $8\delta$  upstream, at a height of  $0.15\delta$ , the grey shadow indicating the path of the jet. In Figure 6a there is clear low-speed circulation behind the jet, while in Figure 6b, the streamlines wind neatly around a single coherent vortex.

Our validation results demonstrate reasonable agreement with the PIV results of Gopalan et al. [7], and provide a good foundation for the pitched and skewed model. Existing literature on low  $VR$  pitched and skewed JICF makes no mention of the vortical shell apparent in the perpendicular case, and this is sup-

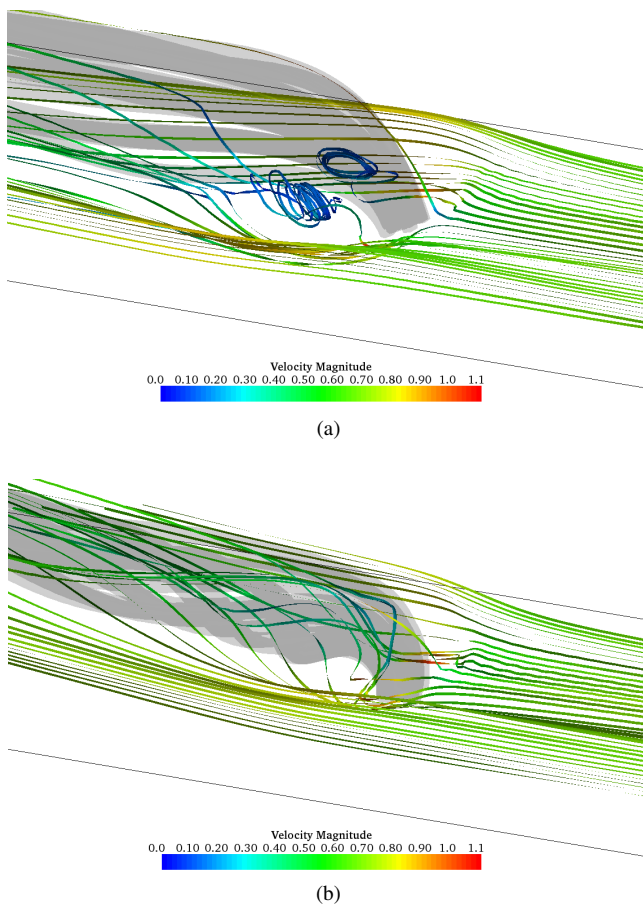


Figure 6: 3D velocity streamlines: (a) perpendicular JICF; (b) pitched and skewed JICF.

ported by our results.

### Summary

The purpose of this work was to investigate the flow structures associated with low  $VR$  pitched and skewed jets in crossflow, in order to understand the underlying mechanism for flow separation control. Two simulations were performed: perpendicular JICF, and pitched and skewed JICF. The low velocity ratio ( $VR < 2$ ), perpendicular JICF results gave good agreement with the available experimental data Gopalan et al. [7], demonstrating the accuracy of the numerical methods used. It was found that weak streamwise reverse-flow immediately behind the jet forms a vorticity 'shell' layer. On the other hand, pitched and skewed jet case results indicated no sign of such a vortical shell, consistent with the literature. To the best of authors' knowledge, this is one of the first published numerical simulations of a low  $VR$  pitched and skewed jet in cross-flow. These results will be further analysed to understand their role in separation delay applications. The present work on a flat-plate boundary layer can be extended to separated boundary layer in order to directly investigate separation control using these jets [19].

\*

### References

- [1] H.H. Pearcey. *Boundary Layer and Flow Control, Vol. 2* (ed. G.V. Lachmann), chapter Shock Induced Separation and its Prevention by Design and Boundary Layer Control. Pergamon Press, 1961.
- [2] M. Gad-el-Hak and D.M. Bushnell. Separation control: Review. *J. Fluids Eng.*, 113:5–30, 1991.
- [3] R.J. Margason. Fifty years of jet in cross-flow research. Technical report, AGARD, National Aeronautics and Space Administration. Ames Research Center, Moffett Field, CA., 1993.
- [4] T. F. Fric and A. Roshko. Vortical structure in the wake of a transverse jet. *J. Fluid Mech.*, 279:1–47, 1994.
- [5] L.L. Yuan, R.L. Street, and J.H. Ferziger. Large-eddy simulations of a round jet in crossflow. *J. Fluid Mech.*, 379: 71–104, 1999.
- [6] J. P. Johnston and M. Nishi. Vortex generator jets - means for flow separation control. *AIAA Journal*, 28:989–994, 1990.
- [7] S. Gopalan, B.M. Abraham, and J. Katz. The structure of a jet in cross flow at low velocity ratios. *Phys. Fluids*, 16: 2067–2087, 2004.
- [8] J. P. Johnston. Pitched and skewed vortex generator jets for control of turbulent boundary layer separation: A review. In *Proceedings of the 3rd ASME/JSME Joint Fluids Engineering Conference July 18-23, 1999, San Francisco, California*, 1999.
- [9] D. A. Compton and J. P. Johnston. Streamwise vortex production by pitched and skewed jets in a turbulent boundary layer. *AIAA Journal*, 30(3):640–647, March 1992.
- [10] R.A. Wallis. A preliminary note on a modified type of air jet for boundary layer control. *ARC Current Papers*, 513: 1–6, 1960.
- [11] G.S. Rixon and H. Johari. Development of a steady vortex generator jet in a turbulent boundary layer. *Trans. ASME*, 125:1006–1015, 2003.
- [12] X. Zhang and M.W. Collins. Nearfield evolution of a longitudinal vortex generated by an inclined jet in a turbulent boundary layer. *Trans. ASME*, 119:934–939, 1997.
- [13] Y. M. Chung. Unsteady turbulent flow with sudden pressure gradient changes. *Int. J. Numer. Fluids*, 47:925–930, 2005.
- [14] T. Grundy. An analysis of the fractional step method for solving the Navier-Stokes equations. Master's thesis, School of Engineering, University of Warwick, U.K., 2008.
- [15] T. S. Lund, X. Wu, and K. D. Squires. Generation of turbulent inflow data for spatially-developing boundary layer simulations. *J. Comp. Phys.*, 140:233–258, 1998.
- [16] J. Jewkes, Y. M. Chung, and P.W. Carpenter. Modifications to a turbulent inflow generation method for boundary layer les. *AIAA Journal*, revised.
- [17] Y. M. Chung, K. H. Luo, and N. D. Sandham. Numerical study of momentum and heat transfer in unsteady impinging jets. *Int. J. Heat Fluid Flow*, 23:592–600, 2002.
- [18] K.E. Meyer, J.M. Pedersen, and O. Ozcan. A turbulent jet in crossflow analysed with proper orthogonal decomposition. *J. Fluid Mech.*, 583:199–227, 2007.
- [19] Y. Na and P. Moin. Direct numerical simulation of a separated turbulent boundary layer. *J. Fluid Mech.*, 374:379–405, 1998.